Design of a Novel Active Multi-Speed Gearbox to Enable Human Muscle-Tendon Performance

Revanth Damerla*, Student Member, IEEE, David Lam, Pranjal Khakse, Qizhang Shen, Kang Yang, and Shorya Awtar, Member, IEEE

Abstract— Matching the attributes of size, weight, strength, speed, and dexterity of human muscle-tendon remains a core challenge in prosthetic and robotic actuator-transmission design, with no existing design having achieved this level of performance at the scale of the human finger. In this work, we present a novel active multi-speed gearbox that enables such performance when combined with a Brushless DC motor. By intentionally incorporating internal resistance, the gearbox allows switching between two reduction ratios using a single lightweight clutch that contributes negligible power to the output, reducing system weight complexity. We analyze two actuator-transmission combinations utilizing this gearbox, each designed to replicate the force, speed, and geometric constraints of the median male index finger metacarpophalangeal (MCP) joint. Both configurations are shown to theoretically meet or exceed the performance of the biological muscle-tendon system in all five attributes. A fabricated prototype demonstrates experimental performance that exceeds muscle-tendon in most of the dynamic range, validating the core concept. These results mark the first instance of a finger-scale actuator-transmission system achieving this level of performance. Future work will focus on further weight reduction, robustness across load cycles, and extension to larger-scale applications such as lower limb prosthetics.

Index Terms—Actuators, biomechatronics, humanoid robotics, mechanical transmissions, prosthetics, variable transmissions

I. INTRODUCTION

ESPITE substantial advances in prosthetic and robotic hardware in the last 20 years, a significant gap remains between their capabilities and those of humans. Prosthetic hands and wrists have yet to match their biological counterparts in all five performance attributes of dexterity, strength, speed, size, and weight [1–4]. Similar challenges exist in humanoid and other robots [5–8]. These persistent challenges indicate that required hardware improvements are not feasible through better optimization of existing actuators and transmissions alone and instead require new innovations.

Much of this challenge is due to the performance gap (e.g. specific torque and power; torque and power density) between human muscle-tendon and existing actuator-transmission combinations [2,9]. Among existing actuator options, Brushless

This research was supported by the Michigan Economic Development Corporation and the University of Michigan through a Michigan Translational Research and Commercialization (MTRAC) grant (Case-392295; Lansing, MI) and the UM Engineering Translational Research (ETR) Fund. Revanth Damerla was supported by a National Science Foundation Graduate Research Fellowship during this research.

DC motors (BLDCs) are the most used because they can achieve larger power densities and specific powers than human muscle. However, to produce required torques, BLDCs are typically paired with transmissions with a single reduction ratio (e.g. gearboxes, screws, linkages). The additional weight and size of these transmissions prevents the articulated joint from matching its human analog in the above five performance attributes. The performance gap of muscle-tendon and BLDC-single transmission systems stems from their differing torque-speed curves: BLDC-fixed ratio systems deliver excess torque at high speeds and excess speed at high torques, requiring oversized actuators that compromise dexterity (Fig. 1a). Thus, muscle-tendon can achieve far higher joint torques and joint speeds relative to the maximum power output.

Significant effort has gone into bridging this gap by leveraging the potential of multi-speed transmissions (i.e. transmissions that can change between multiple reduction ratios, from 2-speed to continuously variable—see Section IIA) [10]. These transmissions better align actuator output with muscle-tendon profiles, thereby supplying the required torque and speed with a smaller, lighter BLDC (e.g. Fig. 1b – a 2-speed example). However, to our knowledge, no actuator-variable transmission combination has matched muscle-tendon in all

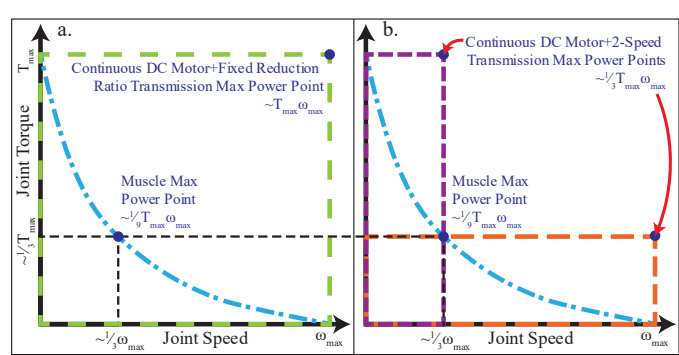


Fig. 1. Torque v. Speed Curve of Joint Driven by Muscle-Tendon (blue) and a BLDC With Two Transmission Options in Continuous Operation and 100% Efficiency: a. BLDC and Fixed Reduction Ratio Transmission (green), b. BLDC and 2-Speed Transmission (orange and purple, depending on ratio). Figure adapted from [11] and muscle curve adapted from [12].

*Revanth Damerla is Corresponding Author: damerla@umich.edu

All authors are with the Precision Systems Design Laboratory, Department of Mechanical Engineering, University of Michigan at Ann Arbor, Ann Arbor, MI 48109 USA.

Color versions of one or more of the figures in this article are available online at http://ieeexplore.ieee.org.

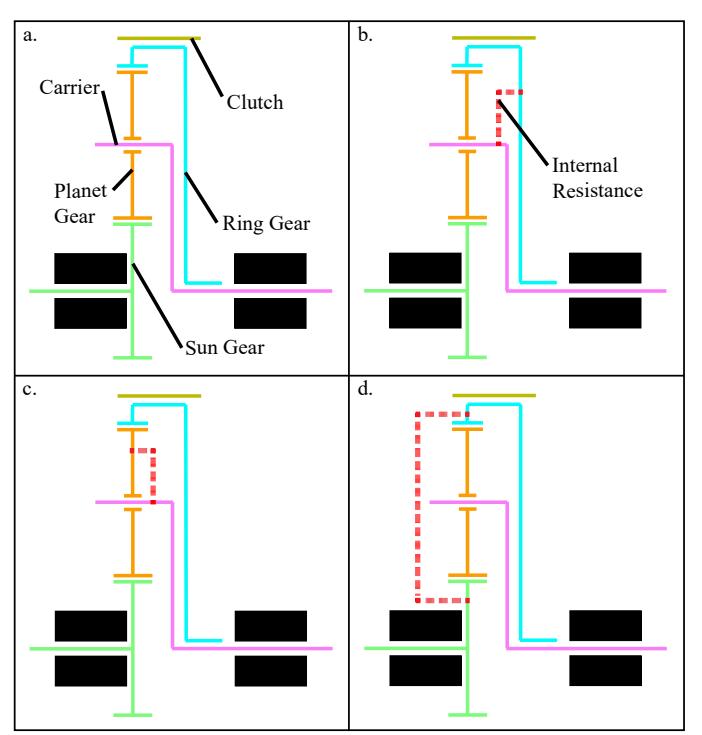


Fig. 2. a. Traditional Planetary Gearbox, b-d. 2-Speed Gearbox with Internal Resistance Between: Carrier and Ring Gear, Carrier and Planet Gears, and Sun and Ring Gears Respectively

five attributes. This limitation has persisted especially at the finger scale, where no actuator-transmission system has matched muscle-tendon in all five attributes.

In this paper, we present the design of a novel multi-speed gearbox, initially described in [13], with the potential to match muscle-tendon performance. The design leverages the intentional inclusion of internal resistance and a lightweight, grounded clutch that enables active switching between reduction ratios with minimal added mass compared to a traditional gearbox. When combined with a BLDC, ball screw, and linkage or cable, the system can match the performance of a median male index finger MCP joint.

The remainder of this paper is structured as follows. Section II presents the motivation for and design of the multi-speed gearbox, including the operating modes, design tradeoffs, and practical implementation considerations. Section III applies the gearbox in two actuator-transmission combinations designed to replicate the median male index finger MCP joint, comparing performance against a muscle-tendon benchmark. Section IV experimentally evaluates a fabricated version of one of these combinations, demonstrating dynamic performance that exceeds muscle-tendon in most of the range. Section V discusses future directions and improvements, including reducing system weight below that of the biological equivalent and extending applicability to other joints.

II. DESIGN OF ACTIVE MULTI-SPEED GEARBOX

A. Motivation for an Active Multi-Speed Gearbox

Although there are many passive multi-speed transmissions

[10,14–26], these options can be challenging to control as they typically change reduction ratio in response to external loading rather than explicit user or controller input. Active multi-speed transmissions are therefore advantageous because the reduction ratio, torque/force, and speed can all be actively controlled.

Existing active multi-speed transmissions designed for relevant applications typically are belt- or cable- [27,28], roller-[29-31], linkage- [11,32-34], gearbox- [35-38], or screw-[39,40] based. Additional examples can be found in [10]. A key limitation in many of these systems is the use of multiple actuators to drive the output, with each requiring its own bearings and support hardware. As a result, the effective actuator specific power is lower than for a single actuator with equivalent combined output power. In contrast, a transmission where a primary actuator produces all the power output while any additional secondary actuators serve only to shift modes with negligible output power can lead to an overall actuatortransmission combination that would weigh far less. However, if the secondary actuators must provide both significant force output and displacement to change reduction ratios (e.g. a dog clutch), they will still be inherently large and heavy. This is especially true if a high engagement force or precise timing is required. Thus, the transmission must only require secondary actuators that either: 1. produce small forces with motion or 2. remain essentially motionless. Feasible options include tooth clutches, electroadhesive clutches, or other such clutches or actuators that can be produced at relatively small scales.

Finally, many multi-speed transmissions are complex and thus inherently not lighter or smaller than single-speed options. Linkages are difficult to utilize in this manner because they occupy larger volumes to allow for movement and are typically used for transmitting larger torques/forces. Screw-based options typically require complex geometries that are large and heavy [35]. While several of the above approaches could, in principle, support this actuator arrangement, gearboxes can typically achieve the highest specific power [2] at lower torque outputs. They therefore offer a favorable combination of compactness and mechanical simplicity, thus motivating the design of an active multi-speed gearbox.

B. Multi-Speed Gearbox Design

We propose a gearbox that incorporates intentional internal resistance (e.g. friction) between components of the gearbox to prevent their relative rotation up to a known torque threshold. For example, in a traditional planetary gearbox (Fig. 2a), friction can be deliberately introduced between the carrier and ring gear (Fig. 2b). When the ring gear is not grounded, the internal resistance causes all components to rotate together, producing a direct drive or 1:1 reduction ratio mode (see Supplementary Video 1). If the applied torque exceeds this threshold, the gearbox transitions out of 1:1 behavior. Before this threshold is reached, a clutch can be engaged to ground the ring gear, activating the nominal gear reduction of the gearbox with the internal resistance subtracted.

Fig. 3 illustrates a two-speed embodiment using a friction pad between the carrier and outer casing (as in Fig. 2b). By

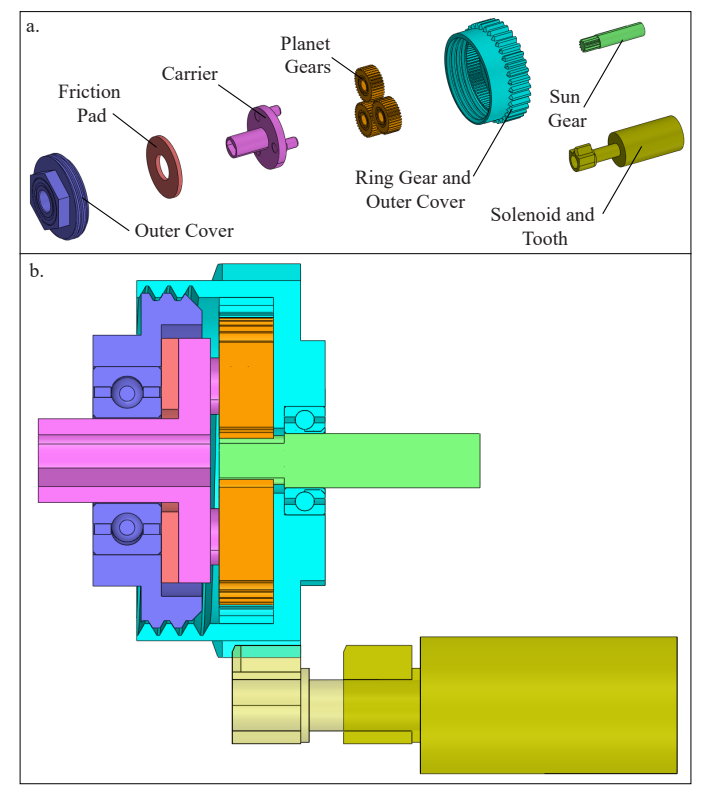


Fig. 3. A 2-speed Embodiment of the Multi-Speed Gearbox with a Tooth Clutch a. Exploded View of the Gearbox and Clutch, b. Cross-section view of the Gearbox and Clutch. Tooth shown both engaged (light yellow – N:1 Mode) and disengaged (dark yellow – 1:1 Mode) with the Ring Gear and Outer Cover

adjusting the pre-load on the friction pad, the internal resistance can be tuned to match desired performance characteristics. Once set, the two halves of the outer cover could be permanently fixed such as with adhesive or a weld. The illustrated embodiment uses a tooth clutch actuated by a small solenoid for clarity, though many other compact actuation methods could be used such as electroadhesive clutches. A single stage of this gearbox made by adding internal resistance to a planetary gearbox leads to the following two modes:

1) Mode 1 - 1:1 Mode or Direct Drive: Ring Gear not Connected to Ground, Internal Resistance not Exceeded

Applying the assumption that the internal resistance of the gearbox prevents the sun gear, ring gear and carrier from rotating relative to each other yields:

$$\omega_{\rm s} = \omega_{\rm c} = \omega_{\rm r} \tag{1}$$

where ω is angular velocity and the subscripts c, s, and r are for carrier, sun gear, and ring gear, respectively. Applying this result to conservation of power under the assumption of 100% efficiency, reasonable for this scenario, with the carrier assumed as the output yields:

$$|P_{in}| = |P_{out}|$$

$$\tau_s \omega_s = \tau_c \omega_c$$

$$\tau_s = \tau_c$$
(2)
(3)
(4)

$$\tau_{\rm s}\omega_{\rm s} = \tau_{\rm c}\omega_{\rm c} \tag{3}$$

$$\tau_{\rm s} = \tau_{\rm c} \tag{4}$$

where P is power and τ is torque.

Next, we examine conservation of linear momentum of the

planet gear, which is assumed to be massless – a reasonable assumption given the magnitude of forces typically applied in a planetary gearbox. Rather than examining a single planet gear, we sum the results of each planet gear, yielding:

$$F_r + F_c + F_s - F_f = 0 (5)$$

where the subscript f refers to the friction pad and F refers to the force applied by a component onto the planet gears. Substituting for torque yields:

$$\tau_r/r_r + \tau_c/r_c + \tau_s/r_s - \tau_f/r_c = 0$$
 (6)

Next, we examine conservation of angular momentum of the planet gear about the center of the gear (again summing the loads applied to all planet gears), which yields:

$$F_s r_p + F_r r_p = 0$$

$$\tau_r = \tau_s \frac{r_r}{r_s}$$
(8)

$$\tau_r = \tau_s \frac{r_r}{r_s} \tag{8}$$

where the subscript p is for planet gear. Combining equations 4, 6, and 8 yields:

$$\tau_{s}/r_{s} + \tau_{c}/r_{c} + \tau_{s}/r_{s} - \tau_{f}/r_{c} = 0$$

$$\tau_{f} = \tau_{s} \frac{2r_{c} + r_{s}}{r_{s}}$$
(10)

$$\tau_f = \tau_s \frac{z_I c_T r_s}{r} \tag{10}$$

A designer will need to decide on an input torque limit after which this 1:1 reduction ratio functionality no longer applies because it will influence the maximum torque output and efficiency in N:1 mode. We designate this input torque limit as $\tau_{lim} = \tau_f \frac{r_s}{2r_c + r_s}$. Any additional input torque τ_s past τ_{lim} will not increase the torque output in 1:1 mode.

2) Mode 2 – N:1 Mode or Alternate Reduction Ratio: Ring Gear Connected to Ground, Internal Resistance Exceeded

The kinematic equation for a planetary gearbox is:

$$\omega_r r_r + \omega_s r_s = \omega_c (r_s + r_r) \tag{11}$$

Since the ring gear is connected to ground and therefore not rotating, we find:

$$\omega_c = \omega_s \frac{r_s}{r_s + r_s} = \omega_s \frac{r_s}{2r_s} \tag{12}$$

 $\omega_c = \omega_s \frac{r_s}{r_s + r_r} = \omega_s \frac{r_s}{2r_c}$ (12) Applying equations 9 and 10 with $\tau_s = \tau_{lim} + \tau_e$, where τ_e is additional applied torque greater than zero, yields:

$$\frac{2\tau_S}{2\tau_S} + \frac{\tau_C}{2\tau_S} - \frac{\tau_f}{2\tau_S} = 0 \tag{13}$$

Tappined torque greater than zero, yields.
$$\frac{\frac{2\tau_{S}}{r_{S}} + \frac{\tau_{C}}{r_{C}} - \frac{\tau_{f}}{r_{c}} = 0}{\frac{2(\tau_{lim} + \tau_{e})r_{C}}{r_{S}} + \tau_{c} - \tau_{lim} \frac{2r_{c} + r_{S}}{r_{S}} = 0}$$

$$\tau_{c} = \tau_{lim} - 2\tau_{e} \frac{r_{c}}{r_{S}}$$
(13)

$$\tau_c = \tau_{lim} - 2\tau_e \frac{r_c'^s}{r} \tag{15}$$

Thus, the torque output is reduced by τ_{lim} , presenting a tradeoff for when to switch between the two modes.

C. Practical Considerations of the Multi-Speed Gearbox

In a planetary gearbox, internal resistance can be introduced between the planet gears and carrier (Fig. 2c), the sun and ring gears (Fig. 2d), and other components based on the discretion of the designer. Supplementary Video 1 provides examples of 2-speed gearboxes with friction pads between the carrier and ring gear (as in Fig. 2b) and planet gears and carrier (as in Fig. 2c). This concept can also extend to other gearbox architectures. For example, friction may be added between the cycloid gear and external gear of a cycloidal drive or between components of other architectures that rotate relative to each other such as in the compound planetary and Ravigneaux gearboxes.

Although friction pads can be made from materials that

enable robust operation for reasonable lifetimes (even millions of loading cycles), they may not be ideal in all applications. One alternative is to alter the tooth profile of one or more gears from the involute curve, causing meshing gears to bind until a known load causes the profile to elastically deform to the involute curve. For example, in a traditional planetary gearbox the ring gear teeth could be altered in this manner. Thus, the planet and ring gears would naturally bind, causing the gearbox to rotate together in 1:1 mode until a specific input torque was applied.

D. Advantages of Proposed Multi-Speed Gearbox

<u>Lightweight</u>: This gearbox-based multi-speed transmission differs from other active multi-speed transmissions in that all output power is supplied by a single primary actuator and only requires a single, lightweight secondary clutch/actuator. This is made possible through the incorporation of internal resistance in the gearbox, which replaces the clutch typically necessary in 1:1 mode. Thus, with the inclusion of a lightweight, low force clutch, it has the potential to be significantly lighter than existing active multi-speed transmission options.

Other recent gearbox-based multi-speed transmissions require the second actuator to produce both substantial force and displacement. For example, [35] utilizes two identical ~200 g actuators with a 100 g gear mechanism to achieve human biceps muscle outputs. While such a design can achieve human joint torques and speed, it does so at a substantially higher weight (i.e. the biceps weigh ~150g, assuming a 1.037 g/cm³ density [41]). In contrast, the proposed multi-speed gearbox requires minimal modifications to a single-stage gearbox and avoids the complex gearing seen in [35–38], resulting in a design that is inherently lightweight at any muscle-tendon scale.

<u>High Specific Torque and Torque Density</u>: Gearboxes provide among the highest specific torques of all transmissions at high speeds and low torques. This makes the proposed gearbox most effective as the first stage after the motor. In this role, tooth loads remain low, enabling a compact, lightweight, and low inertia gearbox (e.g. 1mm face width) while enabling the smallest possible clutch. Thus, the multi-speed gearbox can be paired with transmissions that are better-suited for higher

loads and lower speeds such as ball screws and linkages [2], enabling the smallest possible actuator-transmission with the highest possible specific torque and torque density.

Selectively Backdrivable: Backdrivability offers benefits across many robotic contexts from preventing unpowered locking in upper limb applications to reducing energy usage in swing phase for lower limb applications. Since the entire gearbox spins together in 1:1 mode, the efficiency approaches 100%. Assuming all other transmission elements and the motor are backdrivable, the entire actuator-transmission combination will be backdrivable in 1:1 mode. However, due to the inherent internal resistance, the actuator-transmission will not be backdrivable in N:1 mode. Thus, the system is selectively backdrivable and able to provide the benefits of both options when they are required.

III. APPLICATION OF A 2-SPEED GEARBOX TO REPLICATE THE PERFORMANCE OF THE MEDIAN MALE MCP JOINT

As an exemplary case, we aim to replicate the performance of a median male index finger MCP joint. Grasping generally consists of two phases. In the first phase, digits accelerate to a relatively high speed until they make contact with the object and quickly decelerate (i.e. high speed, low force). In the second phase, the digits apply a large force at a low speed to grasp the object in a stable orientation, only moving to account for the compliance of the digits and the object (i.e. high force, low speed). Thus, a 2-speed gearbox with one reduction ratio meant for each of the two phases of grasping is a reasonable approach.

A. Actuator-Transmission Target Specifications

Two methods are commonly used for actuating the MCP joint in prosthetic hands [1–4]: Method 1. An actuator and transmission housed in the palm or forearm driving the MCP via a cable and Method 2. An actuator and transmission housed in the palm driving the MCP (e.g. via gears or a linkage).

A benchmark of an actuator-transmission combination for Method 1 is the set of four forearm muscles that provide most of the power input to the index finger MCP joint. Table I lists values 1 SD above the mean, which approximate the body

TABLE I
SPECIFICATIONS OF MUSCLES ARTICULATING MEDIAN MALE INDEX MCP AND ACTUATOR-TRANSMISSION COMBINATIONS

Muscle or Actuator-Transmission Combination	Weight (g)	Size - Diameter x Length (mm)	Force (N)	Speed (m/s)	Specific Power (W/kg)
Extensor digitorum communis (EDC)	5.4 ¹	$7.3^3 \times 294$	298	0.34	100^{10}
Extensor indicis propius (EIP)	6.0^{2}	11 ⁴ x 117	9	0.18	110^{10}
Flexor digitorum superficialis (FDS)	13.21	11 ³ x 262	698	0.39	110^{10}
Flexor digitorum profundus (FDP)	17.01	14 ³ x 250	1028	0.37	12010
Target Specifications for Actuator-Transmission Combination for Method 1	41.5	22 ⁵ x 250	1719	0.39	18011
Target Specifications for Actuator-Transmission Combination for Articulating Slider-Crank Linkage for Method 2	41.5	22 ⁶ x 72 ⁷	350	0.18	28011

^{1.} ½ of the weight of each muscle, representing the contribution towards flexing or extending the index finger MCP joint, ^{2.} Full weight of muscle, ^{3.} Calculated from ½ of the muscle PCSA, ^{4.} Calculated from full muscle PCSA, ^{5.} Calculated from the sum of muscle PCSAs, ^{6.} Calculated from ½ of palm width, ^{7.} Calculated from 2/3 of palm length, ^{8.} Calculated from ½ of the muscle PCSA, ^{9.} Calculated from the sum of the FDS and FDP forces, ^{10.} Estimated specific power of the muscle, rather than from the contributions listed in the table, ¹¹ From muscle specific power = ½ *Force*Speed/Weight [9]

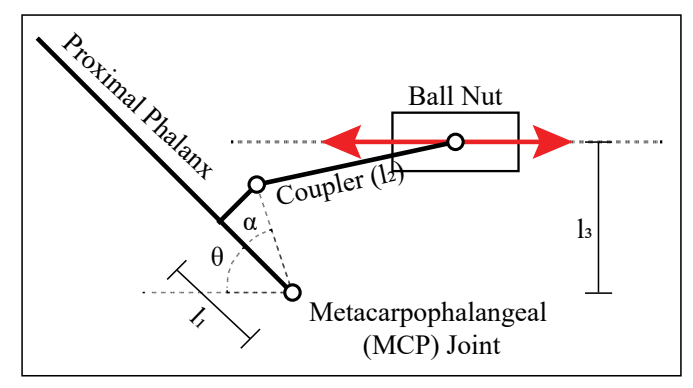


Fig. 4. Slider-Crank Linkage Used in Method 2

$TABLE \ II \\ Dimensions \ of \ Slider-Crank \ Linkage \ Used \ in \ Method \ 2$

Linkage Dimension	Value		
11	13.8 mm		
12	14.5 mm		
1 ₃	6.64 mm		
α	38.7°		

weight of the median American male [42]. The muscle weights were estimated using the only in vivo study measuring forearm muscle volumes we are aware of [41] and assuming a density of 1.037 g/cm³ [9]. Since the EDC, FDS, and FDP each have four muscle bellies – one for each finger – and articulate two independent DoFs (under the assumption that the MCP is independently controlled, and the DIP and PIP are elastically coupled), the weights listed are ½ of the actual muscle weight – approximately half of one muscle belly. This is an intentional underestimate that also excludes the weights of the tendons.

The maximum force is based on the maximum force per unit cross-sectional area of 350 kN/m² [9,12] and the measured Physiologic Cross-Sectional Area (PCSA) of the FDS and FDP – the muscles principally involved in MCP flexion. To maintain a conservative estimate given the hand's intrinsic muscles contribute to flexion of the MCP joint, our target specification is 1/4 rather than 1/8 of the PCSAs of the two muscle bellies. Finally, although the maximum speed of human muscle can reach as high as 5 lengths/s [9], we estimate the maximum speed at 1.5 lengths/s due to finger joint speeds [1] and reasonable lever arms. Given muscle's maximum power output can be estimated as 1/3 of maximum force and 1/3 of maximum speed [9], the target specifications correspond to a specific power of 180 W/kg. Since this value is close to the human muscle maximum value of 200 W/kg, these target specifications are at the very high end of reasonable estimates.

Among actuator-transmission options that can be employed in Method 2, we have previously demonstrated the promise of the BLDC-planetary gearbox-ball screw-linkage actuator-transmission pathway [2] for its combination of high mechanical advantage, specific torque, and specific power. A simple slider-crank linkage (see Fig. 4) was used to convert

linear screw motion into MCP joint rotation due to its compact and lightweight design. The dimensions of the slider-crank linkage listed in Table II were selected based on the median male hand [1]. The maximum force value in Table I is derived from the maximum output force required to achieve the median male proximal phalanx grasp force of 98.8 N [43]. The variable lever arm of the linkage across the 90° range of motion results in greater specific power demands than fixed-lever-arm systems like Method 1 or muscle-tendon units.

B. Actuator-Transmission Combination Design

Given the dimensional constraints, we selected the T-motor 2008 frameless BLDC motor [44] (see Table III) for its high power density, specific power, and specific torque relative to other commercially available actuators [45–50]. Although the BLDC is rated for up to 8000 rpm, most ball screws are only rated for ~6000 rpm. Therefore, unless a downstream gear stage is required, we limit the BLDC to 6000 rpm in 1:1 mode. Finally, the BLDC is rated for 0.020 Nm continuously but can theoretically achieve 0.030 Nm intermittently (i.e. for at least 10 seconds).

1) Actuator-Transmission Combination Design for Method 1

Similar to Method 2, the configuration consists of a BLDC-2-speed gearbox-ball screw-cable. Based on standard ball screws leads of 0.5mm, 1mm, 2mm, and 4mm [51-55], the target of 0.39 m/s is only feasible with a 4mm lead when the 2speed gearbox is in 1:1 mode (see Table IV). Assuming a 90% ball screw efficiency [51–55], the target force is only feasible in N:1 mode with ≥ 6:1 reduction. Using 120 DP gear teeth yields a feasible maximum ratio of 8:1, corresponding to a compact ~22 mm OD gearbox. This high ratio maximizes force output and acceleration in 1:1 mode (i.e. highest possible τ_{lim}), allowing some grasping tasks to be completed without shifting. While a high reduction ratio also corresponds to the slowest possible maximum speed in N:1 mode, this is a small cost as N:1 mode will most likely only be required when close to stall. Under these assumptions, we set $\tau_{lim} = 0.0043 \, Nm$, corresponding to a maximum force of 6.1 N in 1:1 mode. Since the motor can reach 8000 RPM in N:1 mode, the maximum speed in this mode is 0.067 m/s.

A designer can toggle several parameters such as the reduction ratio and τ_{lim} to achieve different static and dynamic performance (e.g. maximum acceleration and bandwidth). Furthermore, if the target force is only required for 10 seconds, τ_{lim} could be adjusted to 0.013 Nm and the 1:1 mode maximum force output would be 19 N.

Component weights in Table III reflect measured values from a T-Motor 2008 with custom shaft and a prototype 2-speed gearbox that achieve the above target specifications, but further weight and size reductions might be possible through better optimization (see Section IV). Electroadhesive clutches are ideal because of their ≤ 1 g weight, mW power consumption, and ≤ 20 ms switching times at this scale [56,57]. Alternatives [58] including tooth clutches would weigh more (potentially > 10 g), consume watts of power, and take longer to switch on/off.

Component	Method 1 Assembly, Minimum Mass		Method 2 Assembly, Minimum Mass		Fabricated Method 2 Assembly	
	Component Name	Weight (g)	Component Name	Weight (g)	Component Name	Weight (g)
BLDC	T-motor 2008 frameless BLDC with shaft	121	T-motor 2008 frameless BLDC with shaft	121	T-motor 2008 frameless BLDC with shaft	121
2-Speed Gearbox	Custom 2-Speed Gearbox with 8:1 Nominal Reduction Ratio	10	Custom 2-Speed Gearbox with 8:1 Nominal Reduction Ratio	10	Custom 2-Speed Gearbox with 8:1 Nominal Reduction Ratio	171
Clutch	Electroadhesive clutch	<1	Electroadhesive clutch	<1	Solenoid Clutch	5 ¹
Ball Screw	4 mm OD x 4 mm Lead Ball Screw	~101	4 mm OD x 2 mm Lead Ball Screw	~101	6 mm OD x 2 mm Lead Ball Screw	241
Cable or Linkage	Cable	<11	Coupler Link and Ball Nut-Link Connection	41	Coupler Link and Ball Nut-Link Connection	61
Total Weight		34		37		64
Maximum Diameter x		22 x 76 (excluding		22 x 98		22 x 98

$TABLE\ III$ Components of the Actuator-Transmission Combinations for Methods 1 and 2

Length (mm) | cable |

TABLE IV THEORETICAL PERFORMANCE OF THE ACTUATORTRANSMISSION COMBINATIONS FOR METHODS 1 AND 2

Value	Method 1	Method 2	
Maximum Speed in 1:1 Mode (m/s)	0.40	0.20	
Maximum Force in 1:1 Mode (N)	6.1	11	
τ _{lim} (Nm)	0.0043	0.0040	
$\tau_{\rm f}({\rm Nm})$	0.039	0.036	
Maximum Speed in N:1 Mode (m/s)	0.067	0.033	
Maximum Force in N:1 Mode (N)	171	350	

The weight for the ball screw and nut is based off a 4 mm OD x 1mm lead ball screws of similar length [2]; cable weight is measured from a tungsten cable with sufficient load rating. The final weight of the actuator-transmission combination is 34 g, meeting the maximum force, speed, size, and weight of the muscle-tendons that articulate the median male MCP joint and thus enabling the design of a robotic hand that matches the human hand in the above five attributes.

2) Actuator-Transmission Combination Design for Method 2

Ball screws with 2mm and 4mm leads can both reach 0.18 m/s in 1:1 mode. To minimize the reduction ratio while meeting target force, we use the 2 mm lead, which can achieve the target force of 350 N with a motor torque of 0.020 Nm and an 8:1 gearbox. The sizes and weights of the BLDC, gearbox, electrostatic clutch, and ball screw are identical to those used in the actuator-transmission combination for Method 1; the weights of the coupler link and ball nut-link connection are similarly based on the weight of representative fabricated components rated for the required loads. The sizes and weights of these components may be further optimized in the future (see Section IV).

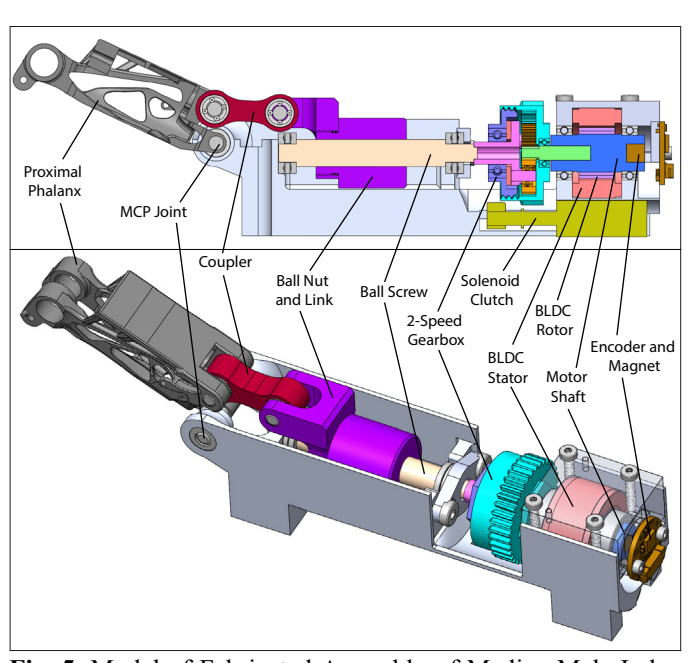


Fig. 5. Model of Fabricated Assembly of Median Male Index Finger MCP Joint a. Cross-Section and b. Angled View with Motor Cover Transparent.

IV. EVALUATION OF PROTOTYPE 2-SPEED GEARBOX IN METHOD 2 ACTUATOR-TRANSMISSION ASSEMBLY

To evaluate the potential of the multi-speed gearbox, we assembled a MCP joint driven by the "Fabricated Method 2 Assembly" actuator-transmission combination in Table III (see Figs. 5 and 6). For simplicity, we used a solenoid tooth clutch instead of the proposed electroadhesive clutch. We also selected a Hiwin® 6mm OD rolled ball screw with RSZ nut (R6-2B1-RSZ). Later, we found that 4mm OD ball screws could achieve the desired load rating of 350 N. These two substitutions are the primary sources of weight difference between the proposed and fabricated Method 2 actuator-transmission combinations.

The 2-speed gearbox (illustrated in Fig. 3) uses one 12-tooth sun gear, three 36-tooth planet gears, and one 84 tooth ring gear

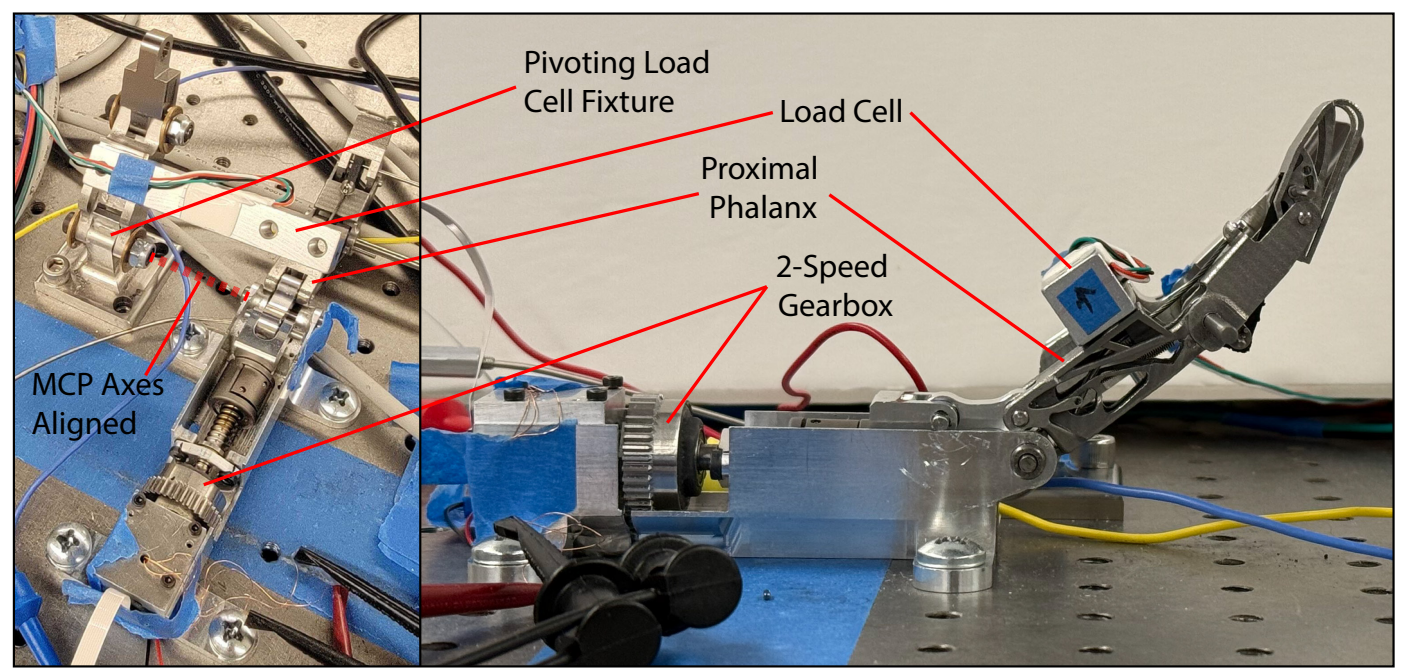


Fig. 6. Experimental setup for the evaluation of the Fabricated Method 2 Assembly.

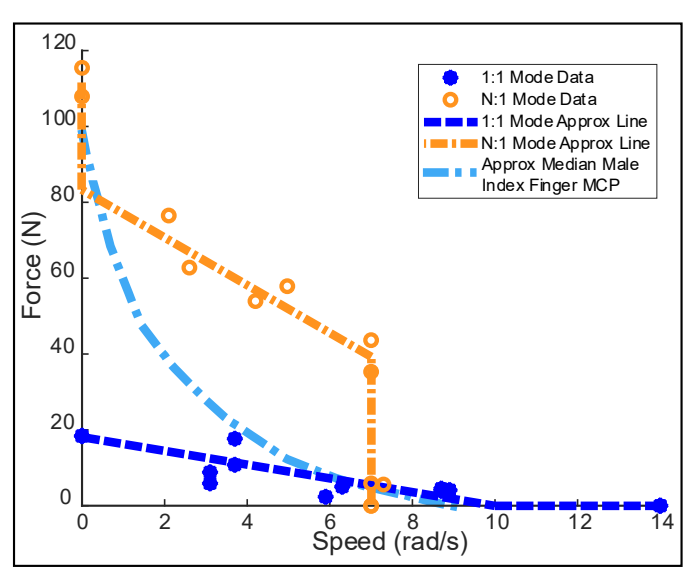


Fig. 7. Force v. Speed of experimental results (with approximate lines) and muscle curve in [12] adapted to the median male index finger MCP joint and proximal phalanx.

all 120 Diametrical Pitch (DP), 0.1875" face width, and 303 stainless steel to balance cost and robustness. The ring gear is integrated into one half of the outer cover for simplicity. After extensive experimentation with methods of producing internal resistance, internal resistance is produced by tightening a friction pad between the gearbox carrier and outer cover. This allows easy adjustment of τ_{lim} via preload by tightening and loosening the outer cover's threaded halves. After testing numerous friction pad materials, a teflon washer was selected for its durability and consistent performance over hundreds of thousands of cycles. The outer cover has teeth on its exterior to engage with the clutch to switch between 1:1 and N:1 modes.

The BLDC is driven by a Nanotec® CL4-E-2-12-5VDI

driver, with feedback from a Renishaw RMB14, 2048 CPR encoder and associated magnet and power from a 24 V benchtop power supply with a rated maximum current of 3.2 A. The driver was operated under closed-loop velocity control. A 5 V output from the driver was used to power the solenoid clutch to shift between 1:1 and N:1 modes.

The three phalanxes of the finger are 3D-printed 17-4 PH. Each phalanx is optimized to minimize weight while ensuring loading remains below an estimated endurance limit of 350 MPa. The finger weighs 41 g, approximately the median male index finger weight and therefore a representative inertia.

Joint speed was measured from video taken with an iPhone 16 Pro at 60 frames per second (see Supplementary Video 2) using Adobe Premiere Pro by tracking MCP angles across three frames centered at approximately 45°. Phalanx force was measured with a calibrated 20 kg cantilever load cell mounted to a pivoting load cell fixture aligned with the MCP axis (see Fig. 6). For static tests, the MCP pivot was locked at 45° and the motor was driven from full extension to stall at max velocity. The phalanx was held for over 10 seconds to ensure a stable continuous force reading, rather than intermittent. At least five measurements were taken at stall and no-load in both N:1 and 1:1 modes. Nearly identical values were consistently obtained for no-load speed in both modes and stall force in 1:1 mode as shown in Fig. 7. N:1 mode stall force had greater variation, likely the result of small variations in the friction pad.

Dynamic testing was conducted with the MCP pivot tightened to a set torque for contact at 15° from extended to provide room for the phalanx to accelerate. The motor was again commanded from fully extended to flexed at the maximum velocity. A constant resistive torque was confirmed by the load cell (see Supplementary Video 2). Four discrete resistive torques were each tried twice between the respective stall and no-load conditions. Only two dynamic measurements

were taken at each torque level due to longer setup and motion execution times. Despite this, the results show consistent trends supporting the validity of the torque-speed profiles and providing a comprehensive picture of the torque-speed curves for both N:1 and 1:1 modes as shown in Fig. 7. An approximate line of the torque-speed curve is drawn for each mode in Fig. 7.

With the 1:1 mode stall force measurement and assuming a ball screw efficiency of 90%, the gearbox had $\tau_{lim} = 0.0119 \ Nm$. Although higher than the value in Table IV, this value closely corresponds to the τ_{lim} value (0.0129 Nm) required for the rated peak motor torque of 0.03 Nm to achieve a maximum proximal phalanx force of 98.8 N in N:1 mode. The higher measured stall force of 117 N in N:1 mode shows that the motor rated peak current is lower than observed and demonstrates the flexibility a designer has when tuning τ_{lim} to achieve their desired performance. Additional friction could be added if a higher 1:1 mode stall force was desirable or could be adjusted in other ways to improve dynamic performance.

Using the simplifying assumption that the muscle force-velocity curve [12] translates to the median male index finger proximal phalanx force and MCP joint speed, we can construct the light blue curve shown in Fig. 7. The results show that this actuator-transmission combination exceeds muscle-tendon performance across nearly the entire operating range, except in the very low-speed, high-force region that is unlikely to feature prominently in typical use. Decreasing τ_{lim} could remove this deficiency, though it would reduce stall force in 1:1 mode. Notably, the stall force and speed capabilities in both modes, except N:1 at low speed, are far higher than necessary. Given these observations, a lighter and smaller motor could have been selected, further reducing the weight and size of future versions.

The fabricated assembly was not optimized to reduce weight and size and could easily be improved in several areas. Firstly, the 2-speed gearbox and linkage have endurance limit safety factors > 5. Furthermore, using an electroadhesive clutch would significantly reduce clutch weight and power consumption. Finally, selection of a smaller and lighter BLDC and ball screw would provide substantial reductions since the BLDC also limited the overall assembly OD. Together, these improvements could dramatically reduce the assembly weight and size to realize the projected values listed in Table III and ultimately match human muscle-tendon in a smaller size and weight.

V. CONCLUSION AND FUTURE WORK

This work presents the first actuator-transmission combinations (i.e. BLDC, 2-speed gearbox, and ball screw with cable or linkage) at finger scale with the potential to match the force, speed, torque, size, and weight of the muscle-tendons that drive a finger. The proposed configurations for both Method 1 and Method 2 meet these benchmarks theoretically, and importantly, do so within a smaller size and weight than their biological counterparts. To our knowledge, no prior system at this scale has demonstrated such performance potential.

Experimental validation of a non-optimized Method 2 assembly confirms the viability of the multi-speed gearbox concept. Despite being intentionally overdesigned for safety

and constructed from heavier components, the fabricated system demonstrated dynamic performance that exceeds the biological muscle-tendon unit across almost all of the operating range. While performance in the low-speed, high-force region remains limited, the experimental data affirm the underlying premise: a single BLDC motor, coupled to the proposed multispeed gearbox, can match or surpass muscle-tendon behavior.

Looking forward, the projected weights for both Method 1 and Method 2 remain well within reach. With appropriate reductions in motor and ball screw size, integration of a lightweight clutch, and further optimizations of the transmission (e.g. smaller safety factors), future versions are expected to meet all five biological attributes. Such reductions are not speculative: the current prototype already achieves them in all dimensions except weight, and the path to that final improvement is clearly defined. These actuator-transmission combinations also illustrate a path to an articulated finger PIP and DIP, potentially utilizing Method 1.

Beyond the hand, this actuator-transmission architecture opens new opportunities in other high-performance end effectors from parallel jaw grippers to highly dexterous soft robots. Other applications include powered lower limb prosthetics, where both higher torque and speed are required simultaneously as opposed to the two-phased nature of grasping (i.e. only requiring high torque near stall and high speed near no-load). Although internal resistance introduces power losses in such dynamic regimes, the associated reduction in motor size and weight may compensate for these drawbacks. Additional experimental evaluation and thermal modeling will be required to explore these tradeoffs fully. Nevertheless, the multi-speed gearbox described here represents a promising path toward achieving human-equivalent actuation in both upper and lower limb prosthetic and robotic systems.

REFERENCES

- [1] Damerla, R. *et al.*, 2021, "A Review of the Performance of Extrinsically Powered Prosthetic Hands," *IEEE Trans Med Rob Bionics*, 3(3), pp. 640–660. doi: 10.1109/TMRB.2021.3100612.
- [2] Damerla, R. et al., 2022, "Design and Testing of a Novel, High-Performance Two DoF Prosthetic Wrist," *IEEE Trans Med Rob Bionics*, 4(2), pp. 502–519. doi: 10.1109/TMRB.2022.3155279.
- [3] Bajaj, N. M., Spiers, A. J., and Dollar, A. M., 2019, "State of the Art in Artificial Wrists: A Review of Prosthetic and Robotic Wrist Design," *IEEE Trans Rob*, 35(1), pp. 261–277. doi: 10.1109/TRO.2018.2865890.
- [4] Belter, J. T., Segil, J. L., Dollar, A. M., and Weir, R. F., 2013, "Mechanical Design and Performance Specifications of Anthropomorphic Prosthetic Hands: A Review," *J Rehab Res Dev*, 50(5), pp. 599–618. doi: 10.1682/JRRD.2011.10.0188.
- [5] Billard, A., and Kragic, D., 2019, "Trends and Challenges in Robot Manipulation," Science, 364(6446). doi: 10.1126/science.aat8414.
- [6] Kootstra, G. et al, 2021, "Selective Harvesting Robotics: Current Research, Trends, and Future Directions," Curr Rob Reps, 2(1), pp. 95–104. doi: 10.1007/S43154-020-00034-1.
- [7] Christensen, H. et al., 2021, "A Roadmap for US Robotics From Internet to Robotics 2020 Edition," Found Trends Rob, 8(4), pp. 307–424. doi: 10.1561/2300000066.
- [8] Custodio, L., and Machado, R., 2020, "Flexible Automated Warehouse: A Literature Review and an Innovative Framework," *Int J Adv Man Tech*, 106(1–2), pp. 533–558. doi: 10.1007/S00170-019-04588-Z.
- [9] Hunter, I. W., and Lafontaine, S., 1992, "Comparison of Muscle with Artificial Actuators," *IEEE Sld-State Sens Act Wksp*, pp. 178–185. doi: 10.1109/solsen.1992.228297.

- [10] Park, J., Lee, J., Seo, H. T., and Jeong, S., 2025, "Variable Transmission Mechanisms for Robotic Applications: A Review," *IEEE Rob Autom Mag*, 32(2), pp. 167–188. doi: 10.1109/MRA.2024.3451795.
- [11] Yang, K., Damerla, R., and Awtar, S., 2022, "Design of a Novel Linkage-Based Active Continuously Variable Transmission for Anthropomorphic Prosthetic and Robotic Hands," *IEEE/ASME Adv Int Mechatronics*, pp. 1–7. doi: 10.1109/AIM52237.2022.9863415
- [12] Zajac, F., 1989, "Muscle and Tendon: Properties, Models, Scaling, and Application to Biomechanics and Motor Control.," *Crit Rev Biomed Eng*, 17(4), pp. 359–410.
- [13] Damerla, R., 2024, "Gear Set," PCT Patent Application WO2024086083A1.
- [14] Shin, Y. J., Lee, H. J., Kim, K. S., and Kim, S., 2012, "A Robot Finger Design Using a Dual-Mode Twisting Mechanism to Achieve High-Speed Motion and Large Grasping Force," *IEEE Trans Rob*, 28(6), pp. 1398– 1405. doi: 10.1109/TRO.2012.2206870.
- [15] Takaki, T. et al., 2015, "Electromyographic Prosthetic Hand Using Grasping-Force-Magnification Mechanism with Five Independently Driven Fingers," Adv Rob, 29(24), pp. 1586–1598. doi: 10.1080/01691864.2015.1079502.
- [16] Singh, H., Popov, D., Gaponov, I., and Ryu, J. H., 2016, "Twisted String-Based Passively Variable Transmission: Concept, Model, and Evaluation," *Mech Mach Theory*, 100, pp. 205–221. doi: 10.1016/J.MECHMACHTHEORY.2016.02.009.
- [17] Horst, R. W., and Marcus, R. R., 2006, "FlexCVA: A Continuously Variable Actuator for Active Orthotics," *Int Conf IEEE Eng Med Bio Soc*, New York, NY, USA, pp. 2425–2428. doi: 10.1109/IEMBS.2006.259950.
- [18] Kim, S., Sim, J., and Park, J., 2020, "Elastomeric Continuously Variable Transmission Combined with Twisted String Actuator," *IEEE Rob Autom Lett*, 5(4), pp. 5477–5484. doi: 10.1109/LRA.2020.3008123.
- [19] Felton, S. M., Lee, D. Y., Cho, K. J., and Wood, R. J., 2014, "A Passive, Origami-Inspired, Continuously Variable Transmission," *Proc IEEE ICRA*, Hong Kong, China, pp. 2913–2918. doi: 10.1109/ICRA.2014.6907278.
- [20] Matsushita, K., Shikanai, S., and Yokoi, H., 2009, "Development of Drum CVT for a Wire-Driven Robot Hand," *IEEE/RSJ IROS*, St. Louis, MO, USA, pp. 2251–2256. doi: 10.1109/IROS.2009.5354239.
- [21] Hirose, S., Ohno, H., Mitsui, T., and Suyama, K., 1999, "Design of In-Pipe Inspection Vehicles for Φ25,Φ50,Φ150 Pipes," *Proc IEEE ICRA*, pp. 2309–2314. doi: 10.1109/ROBOT.1999.770450.
- [22] Takaki, T., and Omata, T., 2006, "100g-100N Finger Joint with Load-Sensitive Continuously Variable Transmission," *Proc IEEE ICRA*, pp. 976–981. doi: 10.1109/ROBOT.2006.1641836.
- [23] Belter, J. T., and Dollar, A. M., 2014, "A Passively Adaptive Rotary-to-Linear Continuously Variable Transmission," *IEEE Trans Rob*, 30(5), pp. 1148–1160. doi: 10.1109/TRO.2014.2333096.
- [24] Ingvast, J., Wikander, J., and Ridderström, C., 2016, "The PVT, an Elastic Conservative Transmission:," *Int J Rob Res*, 25(10), pp. 1013–1032. doi: 10.1177/0278364906069188.
- [25] Schultz, G. R., "End Effector with Load-Sensitive Digit Actuation Mechanisms," U.S. Patent 5,280,981, 1991.
- [26] Hirose, S., Tibbetts, C., and Hagiwara, T., 1999, "Development of X-Screw: A Load-Sensitive Actuator Incorporating a Variable Transmission," *Proc IEEE ICRA*, pp. 193–199. doi: 10.1109/ROBOT.1999.769965.
- [27] Jeong, S. H., Kim, K. S., and Kim, S., 2017, "Designing Anthropomorphic Robot Hand with Active Dual-Mode Twisted String Actuation Mechanism and Tiny Tension Sensors," *IEEE Rob Autom Lett*, 2(3), pp. 1571–1578. doi: 10.1109/LRA.2017.2647800.
- [28] Kembaum, A. S., Kitchell, M., and Crittenden, M., 2017, "An Ultra-Compact Infinitely Variable Transmission for Robotics," *Proc IEEE ICRA*, pp. 1800–1807. doi: 10.1109/ICRA.2017.7989212.
- [29] Brokowski, M. E., Kim, S., Colgate, J. E., Gillespie, R. B., and Peshkin, M., 2008, "Toward Improved CVTs: Theoretical and Experimental Results," *Proc ASME IMECE*, New Orleans, LA, USA, pp. 855–865. doi: 10.1115/IMECE2002-33680.
- [30] Kim, J., Yeom, H., Park, F. C., Park, Y. I., and Kim, M., 2000, "On the Energy Efficiency of CVT-Based Mobile Robots," *Proc IEEE ICRA*, pp. 1539–1544. doi: 10.1109/ROBOT.2000.844815.
- [31] Shin, W., Park, S., Kwon, S., Ahn, B., and Kim, J., 202, "Variable Transmission With Actively Controllable Reduction Ratio," *IEEE/ASME Trans Mech.* doi:10.1109/TMECH.2024.3517540.

- [32] Hur, J., Song, H., and Jeong, S., 2024, "Continuously Variable Transmission and Stiffness Actuator Based on Actively Variable Four-Bar Linkage for Highly Dynamic Robot Systems," *IEEE Rob Autom Lett*, 9(8), pp. 7118–7125. doi: 10.1109/LRA.2024.3418268.
- [33] Lenzi, T., Cempini, M., Hargrove, L. J., and Kuiken, T. A., 2017, "Actively Variable Transmission for Robotic Knee Prostheses," *Proc IEEE ICRA*, pp. 6665–6671. doi: 10.1109/ICRA.2017.7989787.
- [34] Yamada, H., 2012, "A Radial Crank-Type Continuously Variable Transmission Driven by Two Ball Screws," *Proc IEEE ICRA*, pp. 1982– 1987. doi: 10.1109/ICRA.2012.6224866.
- [35] Klas, C., and Asfour, T., 2023, "Reaching Torque-Velocity Profiles of Human Muscles: The Adaptive Cycloidal Linear Drive," *IEEE/ASME Trans Mech*, 28(6), pp. 3470–3479. doi: 10.1109/TMECH.2023.3268556.
- [36] Naclerio, N. D. et al., 2019, "Low-Cost, Continuously Variable, Strain Wave Transmission Using Gecko-Inspired Adhesives," IEEE Rob Autom Lett, 4(2), pp. 894–901. doi: 10.1109/LRA.2019.2893424.
- [37] Sanz-Morère, C. B. et al., 2023, "An Active Knee Orthosis with a Variable Transmission Ratio through a Motorized Dual Clutch," Mechatronics, 94, p. 103018. Doi: 10.1016/J.MECHATRONICS.2023.103018.
- [38] Song, T. G. et al., 2022, "DRPD, Dual Reduction Ratio Planetary Drive for Articulated Robot Actuators," Proc IEEE/RSJ IROS, pp. 443–450. doi: 10.1109/IROS47612.2022.9981201.
- [39] Kober, K., and Rampp, A., 1995, "Multistage Spindle Drive for Converting Rotary Motion into Linear Motion," European Patent 0776285A1.
- [40] Fickler, H., 1982, "Linear Drive Device with Two Motors," Swiss Patent 647,306A5.
- [41] Holzbaur, K. R. S., Murray, W. M., Gold, G. E., and Delp, S. L., 2007, "Upper Limb Muscle Volumes in Adult Subjects," *J Biomech*, 40(4), pp. 742–749. doi: 10.1016/j.jbiomech.2006.11.011.
- [42] C. D. Fryar, Q. Gu, C. L. Ogden, and K. M. Flegal, "Anthropometric Reference Data for Children and Adults: United States, 2011–2014," *Vital Heal. Stat.*, vol. 3, no. 39, 2016.
- [43] J. Lee, "An investigation of finger joint angles and maximum finger forces during cylinder grip activity," Ph.D. dissertation, Biomed. Eng., Univ. of Iowa, Iowa City, IA, USA, 1990.
- [44] "T-MOTOR The Safer Propulsion System." Available: https://uav-en.tmotor.com/.
- [45] "MinebeaMitsumi Brushless Motors," MinebeaMitsumi Inc., Tokyo, Japan. [Online]. Available: https://www.minebeamitsumi.eu/en/brushless-motor/.
- [46] "Faulhaber Drive Systems: 2018," Faulhaber Micromo, Clearwater, FL, USA. [Online]. Available: https://pdf.directindustry.com/pdf/faulhaberdrive-systems-7023.html
- [47] "Maxon Selection Guide: 2019/2020," Maxon Group, Sachseln, Switzerland. [Online]. Available: https://www.maxongroup.co.uk/maxon/view/news/The-new-maxon-catalogue-for-20192020
- [48] "Adamant Namiki Customized Actuator Catalog," Adamant Namiki Precision Jewel Co., Tokyo, Japan. [Online]. Available: https://www.adna.com/en/product/dccorelessmotor/brushlessmotor.html
- [49] "Brushless DC Motors From ElectroCraft," ElectroCraft, Inc., Stratham, NH, USA. [Online]. Available: https://www.electrocraft.com/products/bldc/.
- [50] "Moog Brushless Motors Overview," Moog Inc., Elma, NY, USA. [Online]. Available: https://www.moog.com/content/sites/global/en/products/motors-servomotors/brushless-motors/.
- [51] "Thomson Ball Screws and Ball Splines," Thomson Industries, Inc., Radford, VA, USA. [Online]. Available: https://www.thomsonlinear.com/en/products/ball-screws#literature
- [52] "TBI Motion Ball Screw Catalog," TBI Motion Technology Co., Ltd., New Taipei City, Taiwan. [Online]. Available: https://www.tbimotion.com.tw/en/product/Ball-Screw-SFK/ball-screw SFK.html
- [53] "Misumi Motion Systems Product Catalog," MISUMI Corporation, Schaumberg, IL, USA. [Online]. Available: https://us.misumiec.com/contents/company/about/
- [54] "NSK Ball Screws," NSK Ltd., Shinagawa-Ku, Tokyo, Japan. [Online]. Available: https://www.nsk.com/products/precisionmachine/ballscrew/
- [55] "KSS Standard Products of Ball Screws," KSS Co., Ltd., Ohta-ku Tokyo, Japan. [Online]. Available: https://www.kssballscrew.com/us/download/download.html

- [56] Diller, S., Majidi, C., and Collins, S. H., 2016, "A Lightweight, Low-Power Electroadhesive Clutch and Spring for Exoskeleton Actuation," Proc IEEE ICRA, pp. 682–689. doi: 10.1109/ICRA.2016.7487194.
- [57] Hinchet, R., Shea, H., Hinchet, R., and Shea, H., 2020, "High Force Density Textile Electrostatic Clutch," Adv Mater Technol, 5(4), p. 1900895. doi: 10.1002/ADMT.201900895.
- [58] Plooij, M., Mathijssen, G., Cherelle, P., Lefeber, D., and Vanderborght, B., 2015, "Lock Your Robot: A Review of Locking Devices in Robotics," *IEEE Rob Autom Mag*, 22(1), pp. 106–117. doi: 10.1109/MRA.2014.2381368.



Revanth Damerla and all authors may include biographies if the publication allows. Biographies are often not included in conference-related papers. Please check the Information for Authors to confirm. Author photos should be current, professional images of the head and shoulders. The first paragraph may contain

a place and/or date of birth (list place, then date). Next, the author's educational background is listed. The degrees should be listed with the type of degree in what field, which institution, city, state, and country, and year the degree was earned. The author's major field of study should be lowercase.

The second paragraph uses the preferred third person pronoun (he, she, they, etc.) and not the author's last name. It lists military and work experience, including summer and fellowship jobs. Job titles are capitalized. The current job must have a location; previous positions may be listed without one. Information concerning previous publications may be included. The format for listing publishers of a book within the biography is: *Title of Book* (publisher name, year) similar to a reference. Current and previous research interests end the paragraph.



David Lam and all authors may include biographies if the publication allows. Biographies are often not included in conference-related papers. Please check the Information for Authors to confirm. Author photos should be current, professional images of the head and shoulders. The first paragraph may contain

a place and/or date of birth (list place, then date). Next, the author's educational background is listed. The degrees should be listed with the type of degree in what field, which institution, city, state, and country, and year the degree was earned. The author's major field of study should be lowercase.



Pranjal Khakse and all authors may include biographies if the publication allows. Biographies are often not included in conference-related papers. Please check the Information for Authors to confirm. Author photos should be current, professional images of the head and shoulders. The first paragraph may contain a place and/or date of birth (list place, then

date). Next, the author's educational background is listed. The

degrees should be listed with the type of degree in what field, which institution, city, state, and country, and year the degree was earned. The author's major field of study should be lowercase.



Qizhang Shen and all authors may include biographies if the publication allows. Biographies are often not included in conference-related papers. Please check the Information for Authors to confirm. Author photos should be current, professional images of the head and shoulders. The first paragraph may contain a place and/or date of birth (list place, then

date). Next, the author's educational background is listed. The degrees should be listed with the type of degree in what field, which institution, city, state, and country, and year the degree was earned. The author's major field of study should be lowercase.



Kang Yang and all authors may include biographies if the publication allows. Biographies are often not included in conference-related papers. Please check the Information for Authors to confirm. Author photos should be current, professional images of the head and shoulders. The first paragraph may contain a place and/or date of birth (list place, then

date). Next, the author's educational background is listed. The degrees should be listed with the type of degree in what field, which institution, city, state, and country, and year the degree was earned. The author's major field of study should be lowercase.



Shorya Awtar and all authors may include biographies if the publication allows. Biographies are often not included in conference-related papers. Please check the Information for Authors to confirm. Author photos should be current, professional images of the head and shoulders. The first paragraph may contain a place and/or date of birth (list place, then

date). Next, the author's educational background is listed. The degrees should be listed with the type of degree in what field, which institution, city, state, and country, and year the degree was earned. The author's major field of study should be lowercase.

The second paragraph uses the preferred third person pronoun (he, she, they, etc.) and not the author's last name. It lists military and work experience, including summer and fellowship jobs. Job titles are capitalized. The current job must have a location; previous positions may be listed without one. Information concerning previous publications may be included. The format for listing publishers of a book within the biography is: *Title of Book* (publisher name, year) similar to a reference. Current and previous research interests end the paragraph.